Journal of Power Sources 195 (2010) 3709–3714

Contents lists available at ScienceDirect

Journal of Power Sources

journal homepage: www.elsevier.com/locate/jpowsour

Short communication

Effect of succinic anhydride as an electrolyte additive on electrochemical characteristics of silicon thin-film electrode

Gi-Beom Han[a], Myung-Hyun Ryou[a], Kuk Young Cho[b], Yong Min Lee[c], Jung-Ki Park[a,*]

[a] Department of Chemical and Biomolecular Engineering, Korea Advanced Institute of Science and Technology, 373-1 Guseong-dong, Yuseong-gu, Daejeon 305-701, Republic of Korea
[b] Division of Advanced Materials Engineering, Kongju National University, 275 Budae-dong, Cheonan, Chungnam 303-717, Republic of Korea
[c] Department of Applied Chemistry, Hanbat National University, San 16-1, Deockmyeong-dong, Yuseong-gu, Daejeon 305-719, Republic of Korea

ARTICLE INFO

Article history:
Received 8 September 2009
Received in revised form 5 November 2009
Accepted 22 November 2009
Available online 11 December 2009

Keywords:
Radio-frequency magnetron sputtering
Silicon thin-film electrode
Electrolyte additive
Succinic anhydride
Solid/electrolyte interphase
Lithium battery

ABSTRACT

The effect of an electrolyte additive, succinic anhydride (SA), on the electrochemical performances of a silicon thin-film electrode, which is prepared by radio-frequency magnetron sputtering, is investigated. The introduction of SA into a liquid electrolyte consisting of ethylene carbonate/diethyl carbonate/1 M $LiPF_6$ significantly enhances the capacity retention and coulombic efficiency of the electrode. This improvement in the electrochemical performance of the electrode is attributed to modification of the solid/electrolyte interphase (SEI) layer by the introduction of SA. The differences in the characteristic properties of SEI layers, with or without SA, are explained by analysis with scanning electron microscopy, electrochemical impedance spectroscopy, and X-ray photoelectron spectroscopy.

1. Introduction

There are continuous demands on high-performance lithium secondary batteries for advanced mobile electronic applications. In order to accommodate the need for enhanced cell performance, new electrode materials with higher capacity must be found. Silicon, which has a specific capacity of around 3500 mAh g^{-1} and low charge/discharge potentials of 0.2–0.3 V (vs. Li/Li^+), is one of the most promising candidate materials for a high capacity anode. Despite its strong advantage of high capacity, Si suffers from large volume expansion of up to 300% at the fully-lithiated state [1]. The repeated volume change during cycling results in a sharp capacity decay due to the loss of electric contacts between the Si particles and the conducting agent in porous electrodes [2]. This deterioration in the capacity of Si powder electrodes could be improved by using a proper fabrication method which would include controlling Si particle size, forming composites, and introducing proper binders [2–4]. The repeated surface pulverization with cycles also leads to a decrease in the capacity of Si electrodes, and the subsequent decomposition of electrolyte on the renewed fresh Si surface can be problematic for battery performance [5,6]. On the other hand, it has been also reported that the performance of Si electrodes is highly dependent on the type of electrolyte used in the cell [7,8]. All of the above phenomena are, in principle, related to the interfacial behaviour of Si electrodes. Accordingly, the interfacial properties that are critical in determining the electrode performance must be controlled to achieve a Si electrode of high performance.

One of the well-known approaches to improving the interfacial properties is to introduce additives to the electrolyte that can form a good passivation layer on the surface of the electrode. Despite the many research studies have been conducted on the effect of liquid electrolyte additives on the performance of graphite electrodes [9], there is still limited information about the solid/electrolyte interphase (SEI) layer on a Si electrode. In particular, only a few investigations on the modification of the SEI layer on a Si electrode have been reported, as follows Choi et al. [10] used fluoroethylene carbonate (FEC) as an electrolyte additive and found an enhancement in the cycling performance of a Si thin-film electrode [10]. Chen et al. [11] showed that vinylene carbonate (VC) led to an enhanced cycling performance of a Si film electrode and prevented the decomposition of lithium hexafluorophosphate ($LiPF_6$) salt on the electrode surface [11]. The required nature of the SEI layer on the Si surface includes proper mechanical strength, the ability to prevent the direct contact of the electrolyte with the surface of Si, and stability during extensive cycling.

This study evaluates the effect of an electrolyte additive, viz., succinic anhydride (SA), on the electrochemical characteristics of a Si thin-film electrode. This chemical has been reported to form

* Corresponding author. Tel.: +82 42 350 3965; fax: +82 42 350 3910.
E-mail address: jungpark@kaist.ac.kr (J.-K. Park).

0378-7753/$ – see front matter © 2009 Elsevier B.V. All rights reserved.
doi:10.1016/j.jpowsour.2009.11.142

a stable SEI layer on the anode surface of a cell consisting of graphite and $LiNi_{0.5}Mn_{1.5}O_4$ electrodes [12], but its effect on a Si electrode has still to be, investigated. Electrochemical impedance spectroscopy (EIS), scanning electron microscopy (SEM), and X-ray photoelectron spectroscopy (XPS) are used to investigate the effect of SA on the modification of SEI layers on Si surfaces.

2. Experimental

2.1. Electrode preparation

Radio-frequency (RF) magnetron sputtering was employed to prepare the Si thin-film electrode on copper (Cu) foil (12 μm, Iljin). The base vacuum pressure of the stainless-steel chamber was 3×10^{-5} Torr, and the working pressure was 7×10^{-3} Torr of argon (99.999%). The target used was Si (99.999%) and the target-substrate distance was 7 cm. The Si target was pre-sputtered for 60 min to remove the contaminants on the surface before deposition on copper foil. The thickness of the Si thin film on the Cu foil after 10 min of deposition was determined by a profilometer (ASIQ, KLA Tencor) and found to be about 42 nm. X-ray diffraction analysis (XRD, D/MAX-RC, RIGAKU) was conducted to examine the crystal structure of the Si thin-film electrode.

2.2. Electrochemical measurements

Pouch-type, three-electrode cells were prepared and used in all of the electrochemical performance tests and impedance analyses. The dimensions of both the working electrode (Si thin-film electrode) and the counter electrode (Li metal, 0.1 mm, Honzo) were 2 cm × 2 cm. Cells were fabricated by sandwiching a polypropylene (PP) separator (Celgard 2400, 25 μm) between the Si and Li electrodes. A reference electrode (Li metal, 0.1 mm, Honzo) with an area of 0.1 cm × 0.1 cm was placed between the working electrode and the counter electrode and enclosed in a separator pocket.

The reference electrolyte was 1 M $LiPF_6$ solution in ethylene carbonate (EC)/diethyl carbonate (DEC) (1/1, v/v) which was obtained from Cheil Industry and used as-received. The additive, SA, was purchased from Aldrich and was used without further purification. The amount of SA introduced in the reference electrolyte was 3 wt.%.

A computer-controlled battery measurement system (TOSCAT 3000, Toyo System) was used to conduct charge–discharge tests. The assembled cells were aged for 12 h to saturate the separator with electrolyte and precycled at a constant current of *C*/13, followed by cycling at a constant current of 0.5*C*. Both precycling and cycling were performed in the potential range of 0.005–1.5 V at 25 °C and the initial mode was cathodic alloying of Si with lithium (charge). Ten cells with and without SA in the electrolyte were tested in the experiment for the reliability of the experiment results and the data having a similar initial capacity to the reference cell are reported in the text.

EIS measurements were conducted using a Solartron 1400 frequency response analyzer (FRA) in conjunction with a Solartron 1470E electrochemical interface over a frequency range of 10^6–10^{-1} Hz.

2.3. Surface morphologies and composition analysis

The electrode morphologies of the Si thin films after sputtering, after precycling, and after 100 cycles of charge–discharge were examined by means of a FE-SEM (field emission scanning electron microscope, Sirion, FEI). Analysis of the composition of the SEI layer on Si thin-film electrodes after precycling and 100 cycles was performed using XPS (ESCALAB 250, VG Scientifics). All the high resolution profiles of the XPS data were calibrated with respect to the C 1s peak with a binding energy of 285 eV.

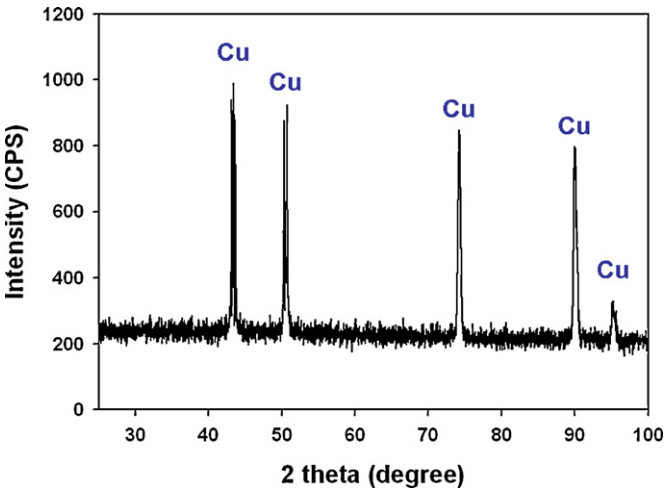

Fig. 1. XRD pattern of Si thin film electrode deposited on Cu foil.

For both SEM and XPS analysis, three independent cells prepared with the same conditions were taken to check the reliability of the data. The Si electrodes from three electrode pouch cells after precycling and after 100 cycles were dismantled and washed in dimethyl carbonate (Aldrich) to remove residual electrolyte solvent and $LiPF_6$ salt, followed by drying in a vacuum chamber for 12 h at room temperature before analysis.

All the electrolyte preparation, cell assembly, disassembly, and electrode washing processes were executed in an Ar-filled glovebox (MOTEK) with water and oxygen contents of 1 ppm.

3. Results and discussion

3.1. Structure of Si thin-film electrode

The XRD patterns for the Si electrodes are presented in Fig. 1. No clear peaks are observed for Si, which indicates that the Si thin film prepared by sputtering is in a totally amorphous phase or in a nano-crystalline state. Similar results have been reported previously [13,14].

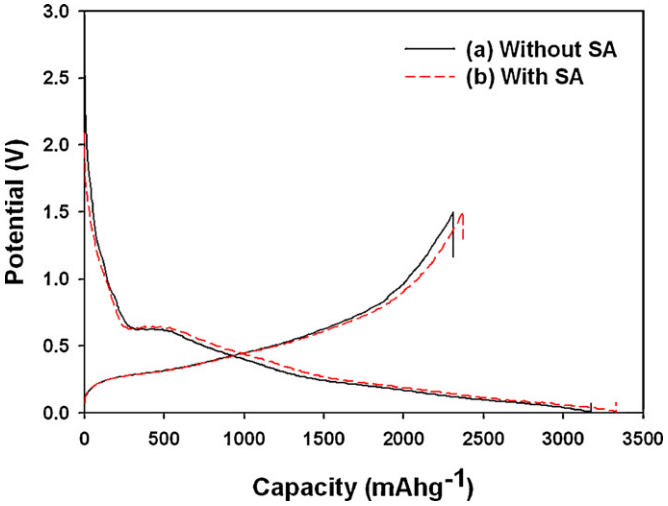

Fig. 2. Charge and discharge profiles of Si thin film electrode during precycling at constant current of *C*/13 (a) without SA and (b) with SA additive in the potential range of 0.005–1.5 V (vs. Li/Li^+).

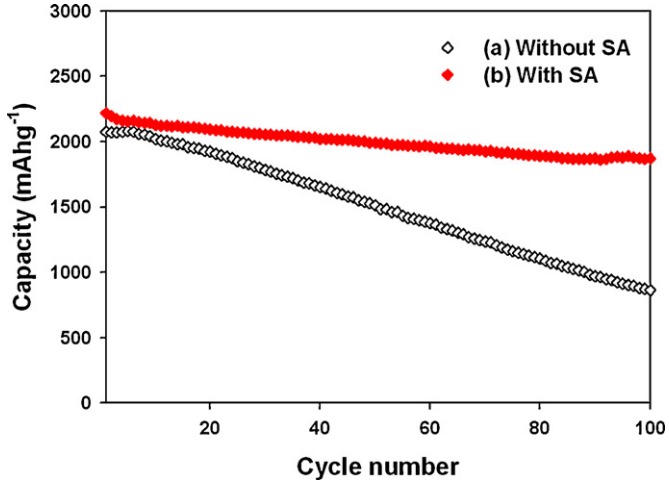

Fig. 3. Discharge capacity retention of Si thin film electrode (a) without SA and (b) with SA additive during cycling tests between 0.005 and 1.5 V (vs. Li/Li^+).

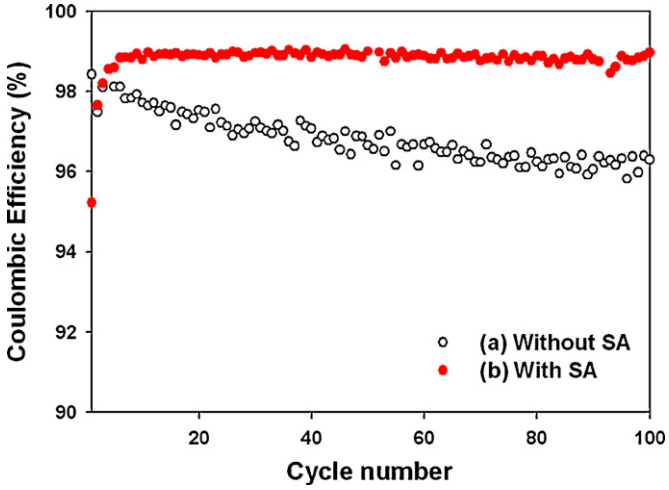

Fig. 4. Coulombic efficiency of Si thin film electrode during cycling tests (a) without SA and (b) with SA.

3.2. Electrochemical performance of Si thin film electrode

The charge and discharge profiles during precycling of the cells under a constant current of *C*/13 are given in Fig. 2. The initial coulombic efficiencies of cells with or without SA during precycling are almost the same (~72%). The initial coulombic efficiency

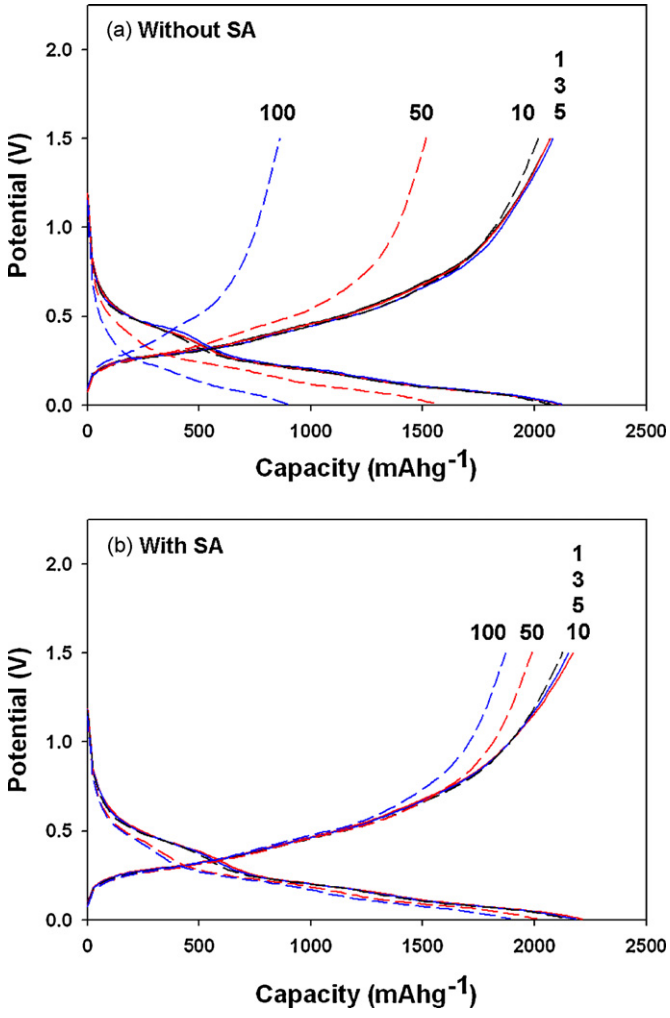

Fig. 6. Charge and discharge profiles of Si thin-film electrodes (a) without SA and (b) with SA at different cycles (1, 3, 5, 10, 50, and 100).

can be directly related to the consumption of lithium ions during precycling, and the ions are mainly consumed during formation of the SEI layer. It is very fortunate that there is no change in the lithium ion consumption even with the addition of SA because it can seriously influence the performance of the complete cell.

The charge–discharge cycling profiles of a Si thin film electrode with or without SA at a constant current of 0.5*C* are shown in Fig. 3. A considerable change in the retention of discharge (de-alloying) capacity is manifested with the introduction of SA during cycling.

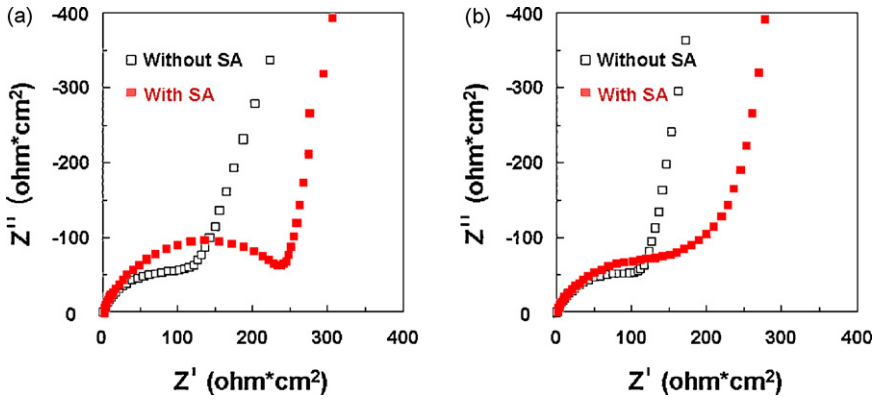

Fig. 5. Nyquist plots for Si thin film electrodes without and with SA (a) after precycling and (b) after 100 cycles.

The discharge capacities after the first cycle of the cell are slightly lower than the discharge capacities during precycling and may result from additional current consumption during formation of the SEI layer in the precycling operation [14]. The discharge capacity of the cell without SA starts to decay only after a few cycles and then steadily continues. It is also found that only around 40% of the discharge capacity with respect to the initial capacity is maintained after 100 cycles of the cell without SA. By contrast, with the introduction of SA, a very significant improvement in the cycling performance of the Si thin-film electrode can be achieved and a discharge capacity of around 1800 mAh g^{-1}, which is about 80% of the initial capacity (2300 mAh g^{-1}), is available even after 100 cycles. than meta-stable lithium alkyl carbonate (Li–OCO_2–R).

The coulombic efficiencies of the cells during cycling are given in Fig. 4. A high coulombic efficiency of over 98% is achieved for the Si electrode without SA at the beginning of cycling, and then decreases to around 96% at the end of cycling. When SA is added to the electrolyte, the coulombic efficiency becomes larger than the initial efficiency during five cycles and then saturates stably with subsequent cycles. From the ability for capacity retention and the changes in coulombic efficiency of Si thin-film electrodes during cycling, it can be suggested that SEI layer formation on the Si electrode in electrolyte without SA additive is almost completed during precycling. By contrast, the characteristics of the SEI layer formed on the Si surface without SA is not sufficiently stable to maintain high coulombic efficiencies. An SEI layer with high stability is formed on the Si electrode with SA additive, and this can enhance the coulombic efficiency during prolonged cycling, even though it takes several more cycles to finalize the development of the SEI layer. The composition of the SEI layer formed on the Si surface in an electrolyte with SA is expected to be rich in stable components such as lithium carbonate (Li_2CO_3) or hydrocarbon, rather

The area-specific impedance spectra of the Si thin-film electrode after precycling and 100 cycles with or without SA are comparatively studied, as shown in Fig. 5. The value of interfacial resistance is found to be almost double in the presence of SA. This indicates that the SEI layer has been modified during precycling, even though there are negligible differences in the coulombic efficiency during precycling. The higher interfacial resistance after precycling is probably related to the stable structure of the SEI layer formed in this stage. After 100 cycles, the interfacial resistance is found to be lower for the electrode without SA in the electrolyte. This is probably due to pulverization of the Si surface and a subsequent increase in surface area [10], which reduces the interfacial resistance. The cycling capacity of the Si thin film electrode is mainly dependent on the loss of silicon caused by pulverization, which is eventually reflected in the cycling performance. The influence of silicon loss is not reflected in the impedance plots.

The operation voltage of a cell is determined by the potential difference between the positive and negative electrodes. Since the Si electrode is a negative electrode, an increase in its potential during discharge (de-alloying) results in a decrease in the overall cell discharge voltage. Fig. 6 presents the capacity–potential profiles of the cells with and without SA at different cycles (1, 3, 5, 10, 50, and 100). As shown, the anodic discharge profile of the Si electrode based on SA introduction at 100 cycles exhibits almost no deviation from the initial profile and a high capacity retention is maintained. This observation is in good agreement with the above cycling performance results.

Scanning electron micrographs of the surface of Si thin-film electrodes are given in Fig. 7. The micrograph in Fig. 7(a) is rep-

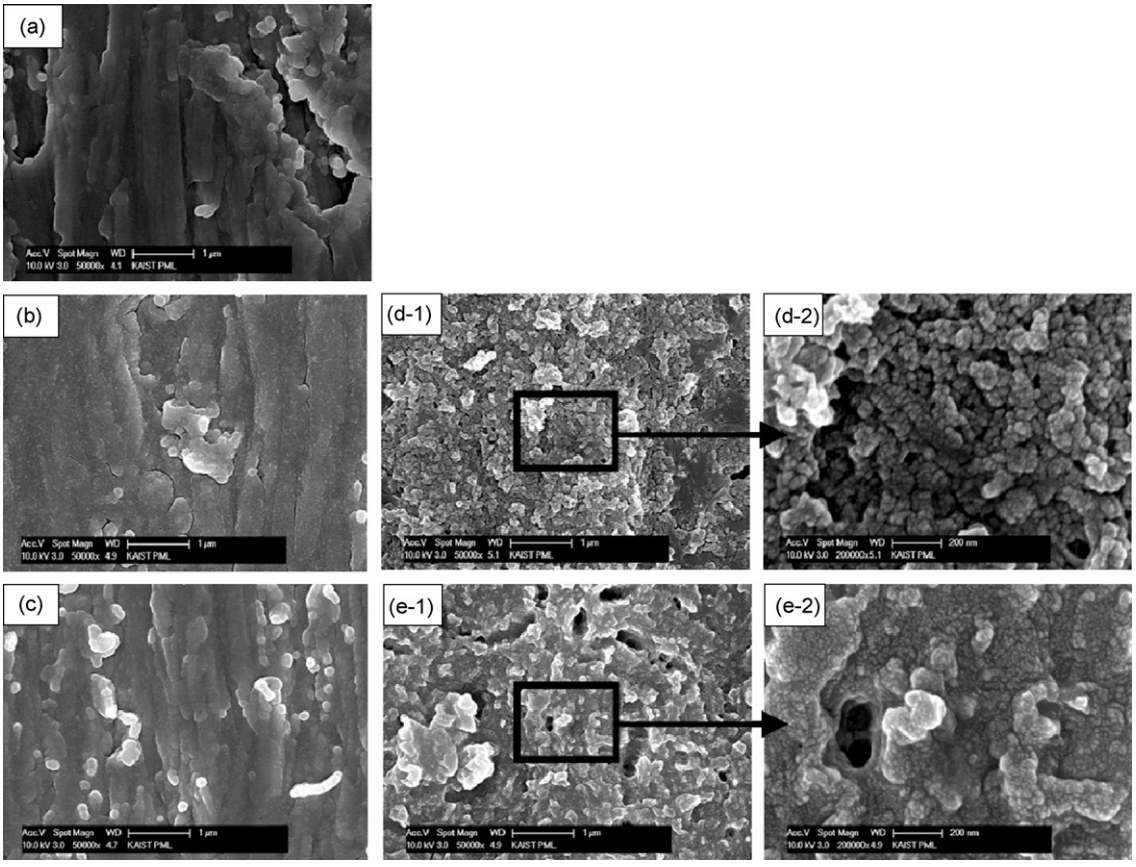

Fig. 7. SEM images of Si thin-film surface (a) after sputtering, after precycling (b) without SA, (c) with SA, after 100 cycles test (d) without SA, and (e) with SA (second images are magnified from the first).

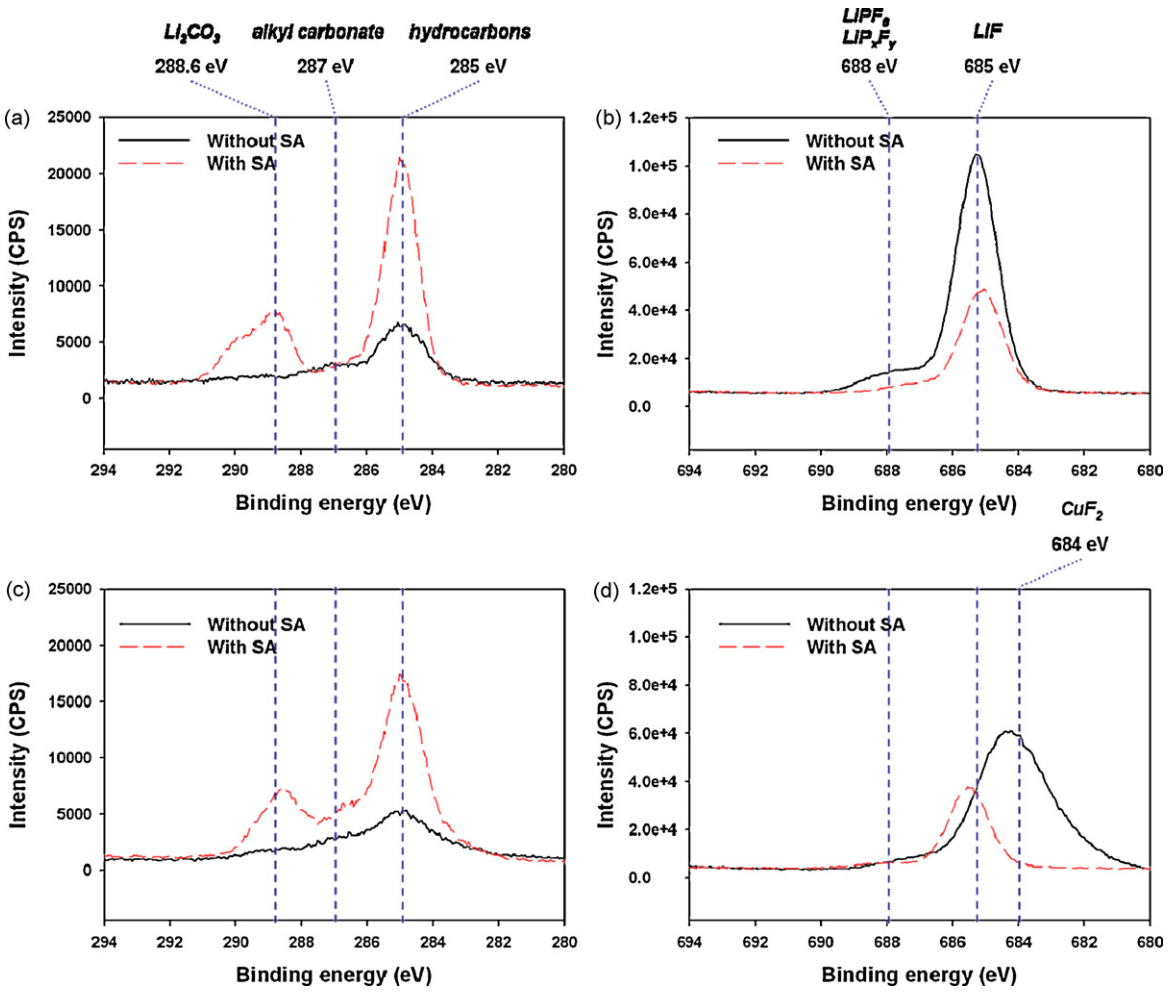

Fig. 8. XPS spectra for Si thin-film electrode (a) C 1s after precycling, (b) F 1s after precycling, (c) C 1s after 100 cycles, and (d) F 1s after 100 cycles.

resentative of the surface of bare Si thin-films prepared by RF magnetron sputtering. There are no significant changes in the surface morphology of the Si electrode after precycling of the cell, as shown in Fig. 7(b) and (c). Characteristic differences in the surface morphology of the Si electrode are observed after 100 cycles. The SEI layer formed on the Si surface without additive has a rougher and more porous morphology than that formed on Si with SA additive. The former morphology may be attributed to the pulverization and repeated SEI layer formation on a fresh Si surface during prolonged cycling. In addition, further decomposition of Li–OCO_2–R in the SEI layer formed in the early stage of cycling to Li_2CO_3 and hydrocarbon can also lead to the development of porous morphology. By contrast, the smooth surface morphology of the SEI layer on the Si surface formed in the cell with SA additive implies that the SEI layer produced in the initial stage of cycling is robust and sufficiently stable to prevent the pulverization and subsequent decomposition of electrolyte on the Si surface. From these results, the composition of the SEI layer formed on the Si surface with SA additive is expected to be rich in stable inorganic components.

3.3. *Effect of SA additive on compositions of SEI layer formed on the Si thin film electrode*

The XPS spectra of Si thin-film electrodes after precycling and 100 cycles are shown in Fig. 8. The C 1s spectra include three peaks corresponding to hydrocarbons at 285 eV, Li–OCO_2–R at 287 eV, and Li_2CO_3 near 289 eV [14,15]. The higher peak intensities of hydrocarbon and Li_2CO_3 after precycling with SA introduction may suggest that the introduction of SA influences the compositional change of the SEI layers formed on the Si surface and promotes the formation of hydrocarbons and Li_2CO_3. The composition of the SEI layer formed with SA introduction after 100 cycles does not change significantly, except for a slight increase in the intensity of lithium alkyl carbonate.

The F 1s spectra show a strong peak from LiF at around 685 eV which is known as a main decomposition product of the PF_6^- anion. The small peak at 688 eV corresponds to $LiPF_6$ and LiP_xF_y [14]. The decrease in the peak intensity at both 685 and 688 eV after precycling with SA introduction implies that the introduction of SA prohibits the decomposition of $LiPF_6$ on the Si surface during precycling. After 100 cycles, the peaks at 685 and 688 eV for the Si electrode based on SA introduction have almost the same intensity. A peak corresponding to lower binding energy near 684 eV, which exists only on the Si surface after 100 cycles without SA introduction, is ascribed to the formation of CuF_2 [16]. The surface of Si thin film electrode is expected to be severely pulverized and delaminated from the copper substrate surface after 100 cycles without SA introduction.

Based on these results, it is suggested that the introduction of SA into the electrolyte promotes the formation of Li_2CO_3 and hydrocarbons, while prohibiting the decomposition of $LiPF_6$ during precycling. The SEI layer formed with the introduction of SA does not undergo significant compositional changes during prolonged

cycling, which can lead to an enhancement of the charge–discharge performance of Si thin-film electrodes.

4. Conclusions

An introduction of a small amount (3 wt.%) of SA into the liquid electrolyte could improve the electrochemical performance of amorphous Si thin film electrode during cycling without sacrificing the charge–discharge potential. This enhancement in the electrochemical performance of a Si thin film electrode is found to be due to the modification of the SEI layer on the Si surface with the introduction of SA additive. The presence of SA can prevent the decomposition of the $LiPF_6$ salt on the Si surface and an SEI layer with higher hydrocarbon and Li_2CO_3 contents is formed on the Si surface. The higher contents of hydrocarbons and Li_2CO_3, and the inhibition of $LiPF_6$ salt decomposition appear to be primary factors for a proper SEI layer which can enhance the interfacial properties of the Si surface.

Acknowledgements

This work was supported by the IT R&D program of MKE/IITA (Core Lithium Secondary Battery Anode Materials for Next Generation Mobile Power Module, 2008-F-019-01).

References

[1] B.A. Boukamp, G.C. Lesh, R.A. Huggins, J. Electrochem. Soc. 128 (1981) 725–729.
[2] J.H. Ryu, J.W. Kim, Y. Sung, S.M. Oh, Electrochem. Solid State Lett. 7 (2004) A306–A309.
[3] H. Uono, B. Kim, T. Fuse, M. Ue, J. Yamaki, J. Electrochem. Soc. 153 (2006) A1708–A1713.
[4] J. Li, R.B. Lewis, J.R. Dahn, Electrochem. Solid State Lett. 10 (2007) A17–A20.
[5] T.D. Hatchard, J.R. Dahn, J. Electrochem. Soc. 151 (2004) A838–A842.
[6] M. Winter, J.O. Besenhard, Electrochim. Acta 45 (1999) 31–50.
[7] I.A. Profatilova, N. Choi, K.H. Yew, W. Choi, Solid State Ionics 179 (2008) 2399–2405.
[8] N. Ding, J. Xu, Y. Yao, G. Wegner, I. Lieberwirth, C. Chen, J. Power Sources 192 (2009) 644–651.
[9] S. Jeong, M. Inaba, R. Mogi, Y. Iriyama, T. Abe, Z. Ogumi, Langmuir 17 (2001) 8281–8286.
[10] N. Choi, K.H. Yew, K.Y. Lee, M. Sung, H. Kim, S. Kim, J. Power Sources 161 (2006) 1254–1259.
[11] L. Chen, K. Wang, X. Xie, J. Xie, J. Power Sources 174 (2007) 538–543.
[12] H. Lee, S. Choi, S. Choi, H. Kim, Y. Choi, S. Yoon, J. Cho, Electrochem. Commun. 9 (2007) 801–806.
[13] L.B. Chen, J.Y. Xie, H.C. Yu, T.H. Wang, Electrochim. Acta 53 (2008) 8149–8153.
[14] Y.M. Lee, J.Y. Lee, H. Shim, J.K. Lee, J. Park, J. Electrochem. Soc. 154 (2007) A515–A519.
[15] K. Kanamura, H. Takezawa, S. Shiraishi, Z. Takehara, J. Electrochem. Soc. 144 (1997) 1900–1906.
[16] C.D. Wagner, W.M. Riggs, L.E. Davis, J.F. Moulder, G.E. Muilenberg (Eds.), Handbook of X-ray Photoelectron Spectroscopy, Perkin-Elmer Corporation, Minnesota, 1979, p. 44.